Interconnect Electromagnetic Modeling using Conduction Modes as Global Basis Functions

Luca Daniel, Jacob White, and Alberto Sangiovanni-Vincentelli.

Abstract— **A new method is formulated for modeling current distributions inside conductors for a quasi-static or a full-wave electromagnetic field simulator. In our method, we model current distributions inside interconnects using a small number of conduction modes as global basis functions for the discretization of the Electric Field Integral Equation. A very simple example is presented to illustrate the potential of our method.**

I. Introduction

As IC's frequencies keep increasing toward the GHz region, quasi-static and full-wave electromagnetic analysis is becoming progressively more important. In particular, signal integrity and electromagnetic interference problems can often result in expensive post-prototype ad-hoc fixes and, sometimes, force the complete redesign of the system layout. In order to avoid these unpredictable additional costs and design time, it is desirable to address EM problems directly during design, for PCBs, packages, as well as IC's.

In this paper, we address the most pressing task: the verification problem. For a verification tool to be effective, it should be able to handle the signal integrity and electromagnetic compatibility verification of the *entire system* (e.g. a printed-circuit board, the IC packages, and the IC power grid). Although fast algorithms have made such analyses much more computationally tractable [1], [2], it is still necessary to keep the number of unknowns to a minimum if full-system analysis is to become fast enough to be used during design.

The most popular method for low-accuracy interconnect and packaging analysis are the PEEC methods [3], [4]. Surface impedance or surface formulation methods have also been considered to try to improve the efficiency of PEEC methods [5], [6], [7]. While many of these methods are quite effective, most of them still require a large number of unknowns to represent skin effects at high frequency. In this paper, we describe a new approach to reducing the number of unknowns required in electromagnetic modeling, by using a very small number of parameters to capture interconnect internal current distributions.

The paper is organized as follows: In Section II we summarize the classical integral equation method. In Section III-A, we derive possible "conduction modes" from the solution of the electric field diffusion equation. Based on such modes, we define in Section III-B global basis functions that we use in Section III-C for the discretization of the Electric Field Integral Equation (EFIE). Finally, in Section IV a very simple example is used to illustrate the computational attractiveness of our method.

Luca Daniel is with University of California, Berkeley. E-mail: dluca@eecs.berkeley.edu

Jacob White is with Massachusetts Institute of Technology. E-mail: white@mit.edu

Alberto Sangiovanni-Vincentelli is with University of California, Berkeley. E-mail: alberto@eecs.berkeley.edu

SRC Task 683.001. SRC Liaisons: Edward J. Bawolek, Intel Corporation Computing Enhancement Architecture Laboratories, Chandler, AZ; Felice Balarin, Cadence Design Systems; Norman Chang, Hewlett-Packard Company; Somnath Viswanath, Advanced Micro Devices, Inc.

II. Background

For a system of conductors embedded in a medium with constant dielectric permittivity and magnetic permeability, the conductor current distribution, $\mathbf{J}$, and the conductor surface charge, ρ, can be determined without computing any fields exterior to the conductors. In particular, the conductor currents can be related to the gradient of a scalar potential, ϕ, using the electric field integral equation

$$\frac{\mathbf{J}(\mathbf{r})}{\sigma} + j\omega\frac{\mu}{4\pi}\int_V \mathbf{J}(\mathbf{r}')\frac{e^{jk|\mathbf{r}-\mathbf{r}'|}}{|\mathbf{r}-\mathbf{r}'|}d\mathbf{r}' = -\nabla\phi \qquad (1)$$

where V is the union of the conductor volumes, $\mathbf{r}$ is a point in V, μ is the magnetic permeability, ϵ the dielectric constant, and $\omega = 2\pi f$ is the angular frequency of the conductor excitation. The scalar potential, *on the conductor surface* can be related to the surface charge through

$$\frac{1}{4\pi\epsilon}\int_S \rho(\mathbf{r}'_\mathbf{s})\frac{e^{jk|\mathbf{r}_\mathbf{s}-\mathbf{r}'_\mathbf{s}|}}{|\mathbf{r}_\mathbf{s}-\mathbf{r}'_\mathbf{s}|}d\mathbf{r}'_\mathbf{s} = \phi(\mathbf{r}_\mathbf{s}), \qquad (2)$$

where S is the union of the conductor surfaces and $\mathbf{r}_\mathbf{s}$ is a point in S.

Since the charge in the interior of the conductor is zero,

$$\nabla\cdot\mathbf{J}(\mathbf{r}) = 0 \qquad (3)$$

for all points r in the *interior* of V. In addition, the current normal to the conductor surface is responsible for the accumulation of surface charge,

$$\hat{\mathbf{n}}\cdot\mathbf{J}(\mathbf{r}_\mathbf{s}) = j\omega\rho(\mathbf{r}_\mathbf{s}) \qquad (4)$$

where $\hat{\mathbf{n}}$ is the unit normal at the point $\mathbf{r}_\mathbf{s}$ on S.

To compute accurate conductor current and charge distributions, or terminal input and coupling impedances, it is necessary to solve the system of integro-differential equations given by (1)-(4). One standard numerical procedure for solving (1)-(4) begins with approximating the volume currents and surface charges by a weighted sum of a finite set of basis functions $\mathbf{w}_j$ and v_j as in

$$\mathbf{J}(\mathbf{r}) \approx \sum_j \mathbf{w}_j(\mathbf{r})I_j \qquad (5)$$

$$\rho(\mathbf{r}) \approx \sum_m v_m(\mathbf{r})q_m. \qquad (6)$$

where I_j and q_m are the basis function weights.

A Galerkin procedure can used to generate a system of equations for the weights. The procedure is to substitute the representations for $\mathbf{J}$ and ρ in (5) and (6) into equations (1) and (2) and then insist that the equation residuals are orthogonal to the basis functions. The result is a matrix equation of the form

$$\begin{bmatrix} R+j\omega L & 0 \\ 0 & P \end{bmatrix} \begin{bmatrix} I \\ q \end{bmatrix} = \begin{bmatrix} V \\ \phi \end{bmatrix} \tag{7}$$

where I and q are vectors of current and charge basis function weights, respectively, and ϕ and V are the vectors generated by inner products of the surface potential or the volume potential gradient with the basis functions. The matrices R, L and P are derived directly from the Galerkin condition and are given by

$$R_{ij} = \frac{1}{\sigma}\int_V \mathbf{w}_i^*(\mathbf{r})\cdot\mathbf{w}_j(\mathbf{r})\,d\mathbf{r} \tag{8}$$

$$L_{ij} = \frac{\mu}{4\pi}\int_V\int_V \mathbf{w}_i^*(\mathbf{r})\cdot\mathbf{w}_j(\mathbf{r}')\frac{e^{jk_0|\mathbf{r}-\mathbf{r}'|}}{|\mathbf{r}-\mathbf{r}'|}d\mathbf{r}'d\mathbf{r} \tag{9}$$

$$P_{lm} = \frac{1}{4\pi\epsilon}\int_S\int_S v_l^*(\mathbf{r})\,v_m(\mathbf{r}')\frac{e^{jk_0|\mathbf{r}-\mathbf{r}'|}}{|\mathbf{r}-\mathbf{r}'|}d\mathbf{r}'d\mathbf{r}. \tag{10}$$

It is possible to tune the discretization to the problem by selecting basis functions which accurately represent the expected current flow and charge density. When discretizing relatively long and thin conductors, and for low accuracy applications, piecewise-constant basis functions are typically used. The functions are generated by covering the surface of each conductor with *panels*, each of which hold a constant charge density. To model current flow, the interiors of all conductors are divided into a 3-D grid of *filaments*. Each filament carries a constant current density along its length and this discretization of the interior captures skin and proximity effects. An example for a section of thin wire is shown in Figure 1.

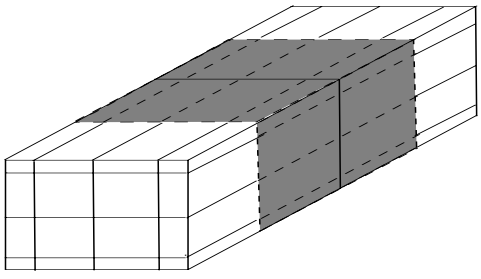

Fig. 1. Discretization of a short section of thin conductor. The volume is discretized into parallel filaments along the length. Surface is discretized into panels shaded in gray.

Once the basis functions have been determined and a Galerkin method is used to discretize (1) and (2), then the current conservation conditions in (3) and (4) must be imposed. There are several approaches for imposing these conditions once the discretization has been established [3], [8], [4].

III. Using conduction modes as current basis functions

Using constant density filaments to discretize the current in the interior of the conductors can produce large linear systems at high frequencies. This is because many filaments will be needed to accurately represent the proximity and skin effects. We present in this Section an alternative choice for the volume discretization, where the basis functions are chosen based on the physical behavior of the current distribution inside the conductors.

A. Conduction modes

Combining the two curl Maxwell differential equations, and using the "good conductor hypothesis" $\sigma \gg j\omega\epsilon$, we obtain the governing diffusion equation for the region inside each conductor

$$\nabla\times\nabla\times\mathbf{E} + j\omega\mu\sigma\mathbf{E} = 0. \tag{11}$$

In terms of the current density, and of the skin depth $\delta = 1/\sqrt{\pi f\mu\sigma}$, we have

$$\nabla\times\nabla\times\mathbf{J} + \left(\frac{1+j}{\delta}\right)^2\mathbf{J} = 0. \tag{12}$$

Let us assume the current flows only in the direction of each conductor's length $\mathbf{J} = J_z\hat{\mathbf{a}}_z$, as in many surface impedance methods, as well as in the Partial Elements Equivalent Circuits (PEEC) method [3]. Let us discretize each conductor only along its length ($\partial J_z/\partial z \approx 0$). Using these assumptions, eq. (12) becomes:

$$\frac{\partial^2 J_z}{\partial x^2} + \frac{\partial^2 J_z}{\partial y^2} - \left(\frac{1+j}{\delta}\right)^2 J_z = 0. \tag{13}$$

Solving the equation for example by separation of variables, we find that a set of physically admissible solutions, or "conduction modes" is [9]

$$J_z^{(\nu)}(x,y) = e^{-p_\nu x}e^{-q_\nu y}, \tag{14}$$

where p_ν and q_ν must satisfy the constraint:

$$p_\nu^2 + q_\nu^2 = \left(\frac{1+j}{\delta}\right)^2. \tag{15}$$

As an illustrative example of a very simple conduction mode, let us choose

$$p_\nu = \frac{1+j}{\delta} \tag{16}$$

$$q_\nu = 0. \tag{17}$$

This mode can account for cross-sectional current distributions decaying exponentially as $1/\delta$ from the edge of the conductor. The left picture in Fig. 2 shows a graphical representation of such current distribution.

The total cross-sectional current distribution can be written as a linear combination of all the conduction modes

$$J_z(x,y) = \sum_\nu C_\nu e^{-p_\nu x}e^{-q_\nu y}. \tag{18}$$

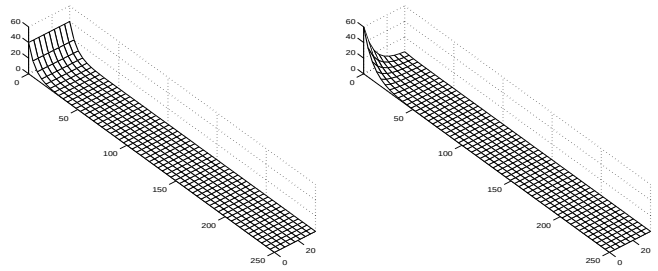

Fig. 2. Graphical representation of a rectangular cross-section "edge mode" (on the left) and of a "corner mode" (on the right). We plot here current density for each point on the cross-section.

Boundary conditions and electromagnetic interactions determine the amplitudes C_ν of each mode. When solving the equations, we should consider the entire infinite set of possible modes. However, in practice, we have found that a very small number of these modes is sufficient to account for the majority of the current distribution. For example, a combination of four simple edge modes, one for each edge, can account for most of the high frequency cross-sectional conductor current distribution. At very high frequency, few other modes need probably to be added to account for corner effects. The simplest example of corner mode is obtained by choosing

$$p_\nu = q_\nu = \frac{1}{\sqrt{2}}\left(\frac{1+j}{\delta}\right) \tag{19}$$

As it is shown in the picture on the right in Fig. 2, this mode can easily account for a cross-sectional current distribution decaying exponentially from the corner of the conductor.

B. Selection of the global basis functions

Let the cross-sectional current density be represented by a collection of global basis functions:

$$\mathbf{J}(\mathbf{r}) = \sum_{j,k} I_{jk}\mathbf{w}_{jk}(\mathbf{r}) \tag{20}$$

where j is a summation index over all the peaces of conductors, and k is a summation index over all the global basis functions chosen for each peace. The conduction modes presented in the previous Section can represent a natural choice for our global basis functions:

$$\mathbf{w}_{jk}(\mathbf{r}) = \begin{cases} \frac{\hat{\mathbf{a}}_{z_j}}{A_{jk}} \sum_\nu e^{\pm p_{jk\nu}(x-x_{jk\nu})} e^{\pm q_{jk\nu}(y-y_{jk\nu})} & \text{if } \mathbf{r} \in V_j \\ 0 & \text{otherwise} \end{cases} \tag{21}$$

where x and y are variables spanning the cross-section of conductor peace j, and refer to one of its corners: $\mathbf{r} = \mathbf{r}_{j_{\text{corner}}} + x\,\hat{\mathbf{a}}_{x_j} + y\,\hat{\mathbf{a}}_{y_j}$. Translation constants $x_{jk\nu}$, $y_{jk\nu}$, and "plus" signs in front of $p_{jk\nu}$ and $q_{jk\nu}$ account for modes decaying from the other corners or edges. We have chosen to introduce a normalization constant A_{jk} defined such that parameter I_{jk} in eq. (20) represent the part of current on the cross-section associated with basis function $\mathbf{w_{jk}}$:

$$A_{jk} = \int_{S_j} \sum_\nu e^{\pm p_{k\nu}(x-x_{jk\nu})} e^{\pm q_{k\nu}(y-y_{jk\nu})} dx\,dy. \tag{22}$$

In order to limit the number of parameters needed to describe the cross-sectional current distribution in each conductor, summation over ν in eq. (21) allows to specify a combination of basic conduction modes into each single basis function. This feature is particularly convenient when modeling PCB traces. In this case, one may wish to combine the lower horizontal edge mode with the upper horizontal edge mode into one single basis function as shown in Fig. 3. In fact the very large aspect ratio of the PCB

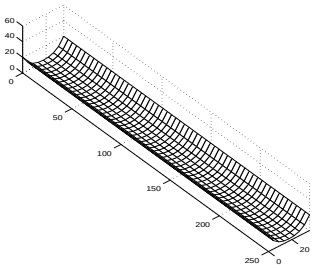

Fig. 3. Example of a global basis function obtained combining two horizontal edge modes. When modeling PCB traces, one can safely assume that there are no significant proximity effect differences between lower and upper modes. Hence, one single basis function can be used to combine for example both horizontal edge modes.

cross-section traces, and the relative large separation between layers, typically do not allow significant proximity effect differences between lower and upper horizontal edge modes. Large differences, instead, can often be observed between any modes on opposite lateral sides (left to right), due to proximity effects. For this reason, for example the two lateral edge modes should be assigned to two separate basis functions.

C. Discretization of the EFIE

Substituting eq. (20) into eq. (1) and using a Galerkin method we obtain:

$$\sum_k R_{ihik} I_{ik} + \sum_{j,k} j\omega L_{ihjk} I_{jk} = \phi_A - \phi_B \tag{23}$$

where we can recognize terms that could be interpreted as equivalent resistances and partial inductances of the conduction modes basis functions

$$R_{ihik} = \frac{1}{\sigma}\int_{V_i} \mathbf{w}^*_{ih}(\mathbf{r}) \cdot \mathbf{w}_{ik}(\mathbf{r})\, d\mathbf{r} \tag{24}$$

$$L_{ihjk} = \frac{\mu}{4\pi}\int_{V_i}\int_{V_j} \mathbf{w}^*_{ih}(\mathbf{r}) \cdot \mathbf{w}_{ik}(\mathbf{r}) \frac{e^{jk_0|\mathbf{r}-\mathbf{r}'|}}{|\mathbf{r}-\mathbf{r}'|} d\mathbf{r}'d\mathbf{r} \tag{25}$$

With our choice of basis functions, the resistance matrix R is a block diagonal matrix. In some cases, e.g. when building Reduced Order Models (ROM), an easily invertible diagonal matrix is more appealing [10], [11]. This

form for R can be obtained by previously orthogonalizing the basis functions.

IV. Example

We are in the process of implementing our new method into a full-wave electromagnetic interference tool. At this point, we can only give a simple example to show the computational properties of the proposed method. We have implemented code to compute the impedance Z of a typical PCB trace 250μm wide, 35μm thick, and 5mm long. Fig. 4 shows the real part of the impedance ($Re\{Z\}$), and the imaginary part divided by $j\omega$ ($L = Im\{Z\}/j\omega$), as a function of frequency. In this example, we have used a classical surface discretization into small panels to account for surface charge, while we have used our conduction-mode global basis functions to account for cross-sectional current density. In particular, we have used these three basis functions:

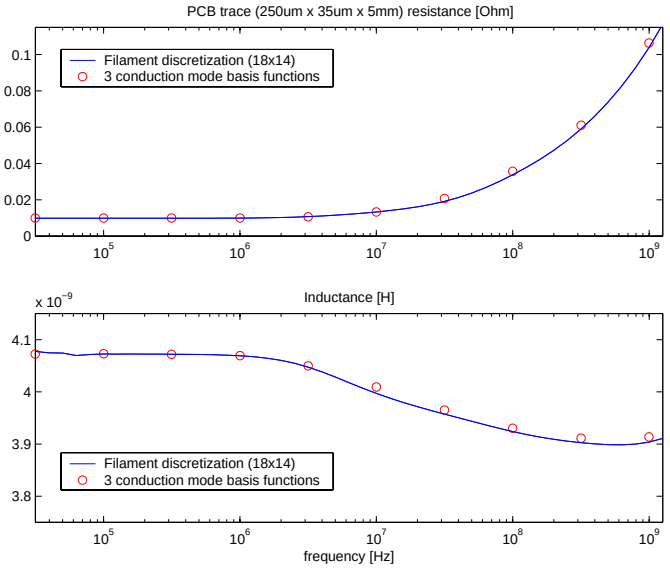

Fig. 4. $Re\{Z\}$ and $L = Im\{Z\}/j\omega$ vs. frequency for a typical PCB trace. The continuous curves are obtained from a classical very accurate 18x14 filaments discretization approach. Circles indicate results from our new method using, in this particular example, only 3 global basis functions.

- one for the left side edge-mode (on the left in Fig. 2);
- one for a similar right edge-mode;
- and one for the combined upper and lower conduction modes shown in Fig. 3.

In Fig. 4, we compared our method with one that uses the same discretization into small panels, and a very accurate cross-sectional discretization into 18x14 small filaments. In the filament approach, we have used thinner filaments close to edges and corners. In particular, as we get closer to edges and corners we keep decreasing the filament thickness by a factor of 1.5.

Compared to the accurate filaments solution, our method shows (in the worst case):

- a 5% error for the resistive part of the impedance $Re\{Z\}$,
- and a (very small) 0.2% error for the inductive part of the impedance $L = Im\{Z\}/j\omega$.

In a second experiment on the same example, we tested the convergence rate of the filaments discretization approach. In this experiment we have observed that, in order to achieve the same errors of our conduction modes method, the filament discretization method requires 10x7 small filaments per cross-section, with filaments thickness decreasing at a ratio of 5 at each step as we get closer to edges and corners. Hence in this example, for the same final accuracy, our method produced a system 20 times smaller than the filament discretization method.

V. Conclusions

In this paper, a new method has been presented for modeling internal conductor current distributions in a quasi-static or full-wave electromagnetic simulator. We have shown how to derive conduction modes, and how to use them as global basis functions for the discretization of the Electric Field Integral Equation. Finally, we presented the potential of our method on a simple example, where linear systems 20 times smaller than the classical filament discretization methods are obtained for the same final accuracy.

References

[1] K. Nabors and J. White. Fastcap: a multipole accelerated 3-d capacitance extraction program. *TCAD*, pages 1447–59, November 1991.

[2] J. R. Phillips, E. Chiprout, and D. D. Ling. Efficient full-wave electromagnetic analysis via model order reduction of fast integral transforms. In *Design Automation Conference*, June 1996.

[3] A. E. Ruehli. Equivalent circuit models for three dimensional multiconductor systems. *IEEE Trans. on Microwave Theory and Techniques*, 22:216–221, March 1974.

[4] M. Kamon, N. Marques, L. M. Silveira, and J. White. Automatic generation of accurate circuit models. *IEEE Trans. on Comp., Packaging, and Manufact. Tech.*, August 1998.

[5] K. M. Coperich, A. E. Ruehli, and A. C. Cangellaris. Enhanced skin effect for partial element equivalent circuit (peec) models. In *IEEE Topical Meeting on Electrical Performance of Electronic Packaging*, October 1999.

[6] J. Wang, J. Tausch, and J. White. A wide frequency range surface integral formulation for 3-d rlc extraction. In *IEEE Internat. Conf. on Computer-Aided Design*, pages 456–460, 1997.

[7] E. Tuncer, B. T. Lee, and D. P. Neikirk. Interconnect series impedance determination using a surface ribbon method. *IEEE Topical Meeting on Electrical Performance of Electronic Packaging*, pages 250–252, November 1994.

[8] N. Marques, M. Kamon, J. White, and L. M. Silveira. A mixed nodal-mesh formulation for efficient extraction and passive reduced-order modeling of 3d interconnects. In *Design Automation Conference*, pages 297–302, 1998.

[9] E. M. Deeley. Surface impedance near edges and corners in three-dimensional media. *IEEE Trans. on Magnetics*, 2:712–714, 1990.

[10] A. Odabasioglu, M. Celik, and L. T. Pileggi. Prima: Passive reduced-order interconnect macromodeling algorithm. *IEEE Trans. on Computer-Aided Design of Integrated Circuits and Systems*, pages 645–654, August 1998.

[11] L. M. Silveira, I Elfadel, M. Kamon, and J. White. Coordinate-transformed arnoldi algorithm for generating guarantee stable reduced-order models of rlc. *Special Issue on Advances of Comp. Methods in Electromagnetics*, pages 377–389, February 1999.